

From Cuprate to Nickelate: Evolution of the Normal State Properties with Ni from $\text{La}_{1.85}\text{Sr}_{0.15}\text{CuO}_4$ to $\text{La}_{1.85}\text{Sr}_{0.15}\text{NiO}_4$

V.L. BEZUSYY^a, A. MALINOWSKI^a, R. MINIKAYEV^a, W. PASZKOWICZ^a, P. DZIAWA^a
AND R. GORZELNIAK^b

^aInstitute of Physics, Polish Academy of Sciences, al. Lotników 32/46, 02-668 Warsaw, Poland

^bInstitute of Low Temperature and Structure Research, PAS, Okólna 2, 50-422 Wrocław, Poland

The influence of Ni doping on the normal-state pseudogap in $\text{La}_{1.85}\text{Sr}_{0.15}\text{CuO}_4$ is studied by dc magnetic susceptibility measurements, accompanied by X-ray powder diffraction analysis and resistivity measurements. The measurements are carried out on the polycrystalline $\text{La}_{1.85}\text{Sr}_{0.15}\text{Cu}_{1-y}\text{Ni}_y\text{O}_4$ samples in the whole doping range from $y = 0.01$ up to $y = 1$. The temperature of pseudogap opening is found to decrease above $y = 0.05$ and to vanish when y exceeds 0.07. At small Ni content, up to $y = 0.07$, the magnetic moment induced by Ni is constant and equal to $0.7 \mu_B$ per Ni, while for larger y it increases abruptly and reaches about $1.6 \mu_B$ per Ni ion for $y = 0.5$. The dependence of the normal-state resistivity on temperature evolves smoothly from the metallic-like for small y , to the variable range hopping, described by the Mott law with the exponent $1/4$, for samples with $y > 0.15$.

PACS numbers: 74.25.Ha, 74.72.-h, 74.72.Kf, 75.30.-m

1. Introduction

The relation of the pseudogap in the normal state of cuprates to the superconducting (sc) gap remains one of the unresolved issues in the physics of strongly correlated systems [1]. Some experiments seem to indicate that the opening of the pseudogap at the temperature T^* is a precursor of the opening of sc gap at T_c [2, 3], some others suggest that the pseudogap competes with the sc gap for the same electrons from the Fermi surface [4].

In-plane impurities intentionally introduced into these materials appear to be a good probe to study the normal-states properties of cuprates [5]. The onset of pseudogap opening T^* is unmodified by Zn substitution, even when the dopant content exceeds this at which sc is completely suppressed [6, 7]. Various microscopic probes suggest a picture of the *local* filling in of the gap in normal-state spin-excitation spectrum by the Zn-induced states taking place in the vicinity of Zn ions, while the spin gap in the regions remote from Zn are unmodified [8, 9]. It is striking that similar picture has been proposed for superconducting properties in the so-called “swiss-cheese” model where superconductivity is suppressed locally around Zn ions and the rest of superconducting “sea” is left intact [10, 11].

In contrast to nominally non-magnetic Zn^{2+} ion ($S = 0$), Ni^{2+} ion in its high-spin state has magnetic moment $S = 1$, and thus has been expected to influence differently the normal-state properties of cuprates. Much to one’s surprise, the effective magnetic moment observed on Ni site is found to be smaller than this induced in Cu–O planes by Zn [12]. The T_c -suppression by Ni is weaker than that of Zn. Muon-spin-relaxation

measurements reveal that Ni, just like Zn, creates the normal-state islands in the superconducting host, but with smaller radius than in the Zn case [13]. Neutron scattering experiments carried out on $\text{La}_{1.85}\text{Sr}_{0.15}\text{CuO}_4$ doped with Ni up to $y = 0.029$ suggest that Ni affects the electronic and magnetic states in the superconducting “sea” outside the nonsuperconducting islands around Ni, in strong contrast to effects of Zn doping [14].

The differences in microscopic pictures of Zn and Ni doping should be reflected in the macroscopic normal-state properties of cuprates and, in particular, in the opening of the pseudogap. This may be probed by the static susceptibility, which is known to decrease below certain temperature T_{\max} as a result of the opening of the pseudogap. So far, most of dc susceptibility measurements of LSCO have been limited to small Ni content, below or just above the Ni content at which superconductivity is suppressed [11, 12, 15]. Early measurements of LSCO with Sr content $x = 0.18$, carried out up to $y = 0.10$, but with T_{\max} extracted only for samples with Ni content $y \leq 0.035$, have resulted in conclusion that the T_{\max} is almost unaffected by Ni [15]. The more detailed later study has found that for small y concentration T_{\max} actually increases with increased y up to critical concentration y_0 ($y_0 \approx 0.015$ for $x = 0.16$) and suggested that Ni atoms are built into system as trivalent ions below this concentration [11]. If so, the observed increase of the T_{\max} means just shifting in the cuprate phase diagram caused by decrease of the concentration of carriers. This explanation, however, has been challenged by the recent X-ray studies, in which no Ni^{3+} state has been found. Instead, it has been suggested that Ni^{2+} acts in LSCO as hole absorber, up to the Ni content equal to the Sr con-

tent in a given system (i.e. $y = 0.15$ for $\text{La}_{1.85}\text{Sr}_{0.15}\text{CuO}_4$, although actually the measurements were carried only up to $y = 0.07$) [16].

Motivated by these conflicting results, in the present work we extend the measurements of the LSCO susceptibility to the larger Ni content, well above this at which superconductivity is suppressed. Extending of Ni doping range eventually leads to $\text{La}_{1.85}\text{Sr}_{0.15}\text{NiO}_4$. The nickelate, LSNO, is isostructural with cuprates LSCO, but superconductivity has never been observed in it. In this context, a systematic examination of evolution of the normal state properties when Cu is replaced by Ni in LSCO may shed some light onto the problem of correlation between the pseudogap in the normal state and superconductivity.

2. Experiment

The polycrystalline samples of $\text{La}_{1.85}\text{Sr}_{0.15}\text{Cu}_{1-y}\text{Ni}_y\text{O}_4$ ($0.00 \leq y \leq 1.00$) were prepared by the standard solid-state reaction method. The powders of 4N–5N pure La_2O_3 , SrCO_3 , CuO and NiO were mixed, pressed into pellets and sintered in flowing oxygen at 1050°C for 48 h. After cooling with the rate of 2°C per 1 min the samples were reground and the procedure was repeated twice.

The diffraction measurements were carried out at the Bragg–Brentano diffractometer (Philips X’Pert Pro Alpha1 MPD, Panalytical) using NIST 640c internal X-ray diffraction standard and the Rietveld-refinement program, Fullprof.2k (ver. 2.70), was used for the structural analysis. The resistivity was measured using the standard dc four-probe method in the 4.2–300 K temperature range. Magnetic susceptibility measurements were carried out using two setups: the commercial SQUID magnetometer (MPMS, Quantum Design) working in the temperature range 2–400 K and the magnetic field up to 5 T, and the home-built setup based on Cryogenics Consultants SQUID sensor and working in the temperature range 1.6–280 K and magnetic field up to 0.3 T.

3. Results and discussion

The X-ray diffraction spectrum reveals that all of the samples up to $y = 0.70\%$ crystallize in tetragonal (space group $I4/mmm$) structure. The specimens are of a good quality and no additional phase is detected. The lattice constants c and a change linearly with Ni content, as displayed in Fig. 1. The c constant decreases with the rate of $6 \times 10^{-3} \text{ \AA}$ (i.e. 0.05% c) per 1% of Ni while a increases with the rate of $8 \times 10^{-4} \text{ \AA}$ (0.02% a) per 1% of Ni. Vegard’s law is fulfilled in the whole doping range. The calculated c/a ratio decreases with increasing y , closely resembling the results reported in Refs. [17, 18]. Neither $a(y)$ nor $c(y)$ dependences show any anomaly around $y = 0.15$, for which the distance between Ni and in-plane O(1) atoms are supposed to change abruptly according to X-ray-absorption fine structure measurements from Ref. [16].

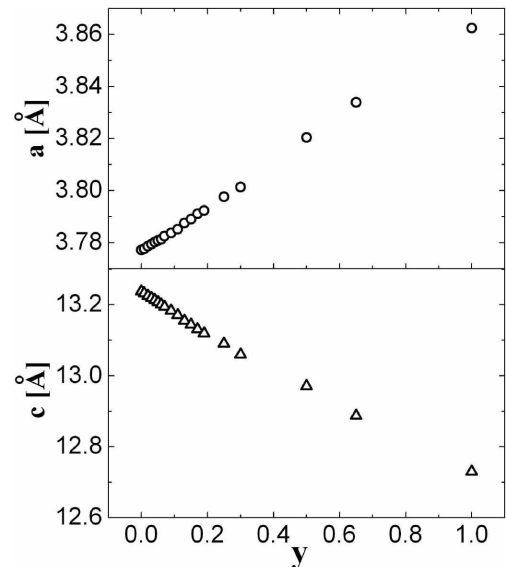


Fig. 1. The lattice parameters of $\text{La}_{1.85}\text{Sr}_{0.15}\text{Cu}_{1-y}\text{Ni}_y\text{O}_4$ as a function of Ni content.

Resistivity measurements reveal that the T_c decreases with increasing Ni content, and drops below 4.2 K when y exceeds 0.04, consistent with previously reported suppression of superconductivity around 0.05 [17]. For small y the resistivity ρ in the normal state is metallic-like and increases linearly with increasing temperature. At higher y the ρ at low T clearly displays insulating behavior. Beginning with $y = 0.15$ sample, the ρ vs. T curves may be fitted with the variable-range hopping formula, $\rho = \rho_0 \exp(T_0/T)^{-\alpha}$, with T -independent prefactor and the exponent $\alpha = 1/4$, which is indicative of 3D hopping processes. This smooth evolution of ρ with y is consistent with that observed in Ref. [17].

The magnetic susceptibility χ vs. T measurements has been measured in a wider temperature window than the resistivity. The data taken at low field of 10 Oe reveal that the superconductivity survives up to $y = 0.054$. In Fig. 2 we show that for small y the T -dependent part of the normal-state magnetic susceptibility, $\chi(T) - \chi_0$, can be decomposed into two terms. One term describes the magnetic behavior of 1/2-spin antiferromagnetic (AF) lattice formed in the Cu–O plane. The second is the Curie term, attributed to the additional magnetic moment introduced by Ni ions. We analyze the first term using the universal empirical curve, proposed without parameterization for LSCO independently by Johnston [19] and Nakano [20]. All $\chi(T)$ vs. T curves for LSCO with various Sr content are found to collapse onto a single universal curve F , when represented in the reduced variables, $(\chi - \chi_0)/(\chi - \chi_{\max})$ and T/T_{\max} , where $\chi_{\max} = \chi(T_{\max})$ is the maximal value of χ . This means that susceptibility can be rewritten as $\chi = \chi_0 + (\chi_{\max} - \chi_0)F(T/T_{\max})$. The attempts to parameterize the curve F did not lead to any microscopic

model [21]. The shape of F for $T > 0.7T_{\max}$ agrees well with the calculations for $1/2$ spin quadratic AF Heisenberg lattice [19]. Below the maximum at T_{\max} , the F is described quite well by Williams' model, according to which $F \sim [1 - \tanh^2(E_g/2k_B T)]$, where E_g is the pseudogap energy and $E_g/2k_B$ is roughly proportional to T_{\max} [9]. However, with the help of this model it is difficult to find a possible evolution of T_{\max} in the case when T_{\max} shifts towards the smaller values inside the accessible measurement window, because the model does not involve the region above T_{\max} . Therefore, we used the universal curve F_{univ} from Ref. [20] (Fig. 6) and fitted the susceptibility data for small y with the formula

$$\chi = \chi_0 + A_{\text{spin}} \times F_{\text{univ}}(T/T_{\max}) + C/T. \quad (1)$$

In Eq. (1) χ_0 is the T -independent part, $A_{\text{spin}} \times F_{\text{univ}}(T/T_{\max})$ is the T -dependent contribution from the magnetic moments in the Cu–O planes forming AF lattice and C/T is the Curie-like term describing the contribution from Ni ions. The T -independent part χ_0 is a sum of three components: the isotropic contribution from the closed Cu shells χ_{dia} , the Van Vleck contribution χ_{VV} , and the contribution from charge carriers, χ_{holes} that includes both the positive Pauli susceptibility and the negative Landau diamagnetic susceptibility. An example of the fit of Eq. (1) to the data for $y = 0.04$ sample is shown in Fig. 2.

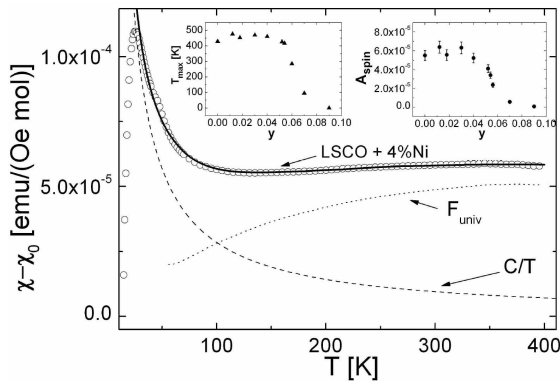


Fig. 2. $\chi(T)$ for $\text{La}_{1.85}\text{Sr}_{0.15}\text{Cu}_{1-y}\text{Ni}_y\text{O}_4$ with $y = 0.04$ Ni content. The solid line represents the best fit of Eq. (1) to the data, with $\chi_0 = 1.003 \times 10^{-4}$ emu/(Oe mol), $A_{\text{spin}} = 5.155 \times 10^{-5}$, $T_{\max} = 460$ K and $C = 2.845 \times 10^{-3}$ emu K/(Oe mol). The dotted line represents the universal curve F_{univ} with the parameters adjusted to match these from the best fit, the dashed line is the Curie term. The insets show the dependence of T_{\max} (left part) and A_{spin} (right part) on the Ni content.

Let us note that for this sample and for others as well, it is not necessary to add any Curie–Weiss constant to obtain very good fits, as it appeared to be essential for $\text{La}_{1.82}\text{Sr}_{0.18}\text{Cu}_{1-y}\text{M}_y\text{O}_4$ (where $M = \text{Ga}, \text{Zn}, \text{Ni}, \text{Co}$) [15]. The left inset to Fig. 2 shows that the T_{\max} is nearly constant for y up to about 0.05. At larger y the T_{\max} starts to decrease abruptly and disappears

above $y = 0.07$. This is accompanied by simultaneous evolution of the coefficient A_{spin} (right inset), which remains almost constant up to $y = 0.03$, starts to decrease slowly for larger y and finally disappears at y larger than 0.07. Both $T_{\max}(y)$ and $A_{\text{spin}}(y)$ dependences indicate that Ni-doping destroys the “magnetic integrity” of the Cu–O planes. Assuming that the doping evolution of T_{\max} mimics the same evolution of T^* , i.e. the temperature of opening of the pseudogap in the normal state, one can clearly see that the pseudogap disappears at y just a bit larger than that at which superconductivity is destroyed. Thus our study reveals that Ni doping affects the temperature T^* of the pseudogap opening. This is in contrast to Zn doping which has no effect on T^* in LSCO, as described in Sect. 1 [7, 22]. As the “swiss-cheese” model proposes, in Zn-doped LSCO superconductivity is destroyed locally and the “robust” normal-states properties (including pseudogap with the same T^*) are restored in the vicinity of Zn ions [10, 11]. The present experiment suggests very different picture of Ni doping, consistent with the “diluting” of the normal-state properties (including pseudogap) in the total volume of the system [11]. The fact that closing of pseudogap follows almost immediately the suppression of superconductivity suggests the relation between the pseudogap and the sc gap.

No A_{spin} part (see Eq. (1)) was found in the susceptibility curves for larger Ni contents, starting from $y = 0.09$. As it is depicted in Fig. 3, for all samples with larger y , up to $y = 0.65$, χ vs. T dependence above ≈ 30 K is well described by the Curie–Weiss function, $C/(T - \theta)$, with negative θ of the order of 10 K. This indicates the presence of AF correlations between the ions. Let us note that the slope of the straight lines fitted to the data changes monotonically with y consistently with Ni content. The parameter C extracted from the fit, combined with the values of C obtained from fitting the data for smaller y to Eq. (1), is shown as a function of y in the inset to Fig. 3. The $C(y)$ dependence is linear up to $y = 0.07$. Thus the magnetic moment induced by Ni is constant in this doping range. The value of the effective magnetic moment extracted from the relation $C = y \times N_A \times p_{\text{eff}}^2/3k_B$ is $p_{\text{eff}} = (0.7 \pm 0.05) \mu_B$ per Ni atom, close to value of $0.6 \mu_B/\text{Ni}$ measured earlier [12]. It has been proposed recently that such a tiny paramagnetic moment may be explained by bonding of holes to Ni ions and forming a state with effective moment $1/2 \mu_B$, i.e. the same as that of surrounding Cu ions [16]. However, this microscopic picture predicts the increase of p_{eff} beginning from y equal to hole concentration in the system, $n = 0.15$ [16], whereas our results indicate that p_{eff} starts to increase abruptly for $y = 0.07$, i.e. at about *half* of hole concentration in the system, $y \approx n/2 = 0.15$.

Finally, let us note that at $y = 0.5p_{\text{eff}}$ reaches about $1.6 \mu_B/\text{Ni}$. This effective value ($p_{\text{eff}} = g[S(S+1)]^{1/2}$) is more consistent with $S = 1/2$ than with $S = 1$ expected for Ni^{2+} ion. Let us note, however, that this value is averaged for *all* Ni ions, in particular these with absorbed

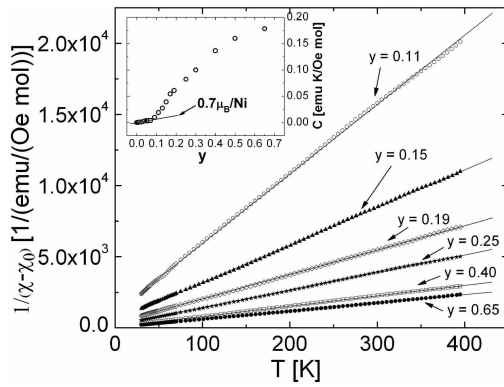


Fig. 3. Inverse of the T -dependent part of magnetic susceptibility for the samples with high concentration of Ni, measured at $B = 1$ kGs. The solid lines are the best fits to the Curie–Weiss function above 30 K. Inset shows the dependence of C on the Ni content, y . The solid line in the inset is the best linear fit up to $y = 0.07$ that gives $\mu_{\text{eff}} = 0.7 \mu_{\text{B}}/\text{Ni}$ ion.

hole. The actual moment that resides at Ni site probably results from the mixed quantum state, being the superposition of low- ($S = 0$) and high- ($S = 1$) spin pure states of Ni ion.

4. Conclusions

Ni doping changes the normal-state properties of LSCO. Resistivity of the system evolves from the metallic-like in samples with small y to the 3D variable-range hopping at sufficiently low temperatures in the samples with high Ni content. The temperature of the opening pseudogap T^* abruptly decreases with y for $y > 0.05$ and the pseudogap disappears above $y = 0.07$. The suppression of T^* with y is consistent with the picture of “diluting” of the magnetic normal-state properties of LSCO by Ni. The observed magnetic moment introduced by Ni at high concentration is closer to that expected for a spin $S = 1/2$ than to that for a spin $S = 1$.

Acknowledgments

This work was supported by funds of the Polish Ministry of Science and Higher Education as a research project for years 2007–2010 (grant No. N202 048 32/1183).

References

- [1] T. Timusk, B. Statt, *Rep. Prog. Phys.* **62**, 61 (1999).
- [2] K. Anagawa, T. Watanabe, M. Suzuki, *Phys. Rev. B* **73**, 184512 (2006).
- [3] Hai-Hu Wen, Xiao-Gang Wen, *Physica C* **460-462**, 28 (2007).
- [4] M. Hashimoto, T. Yoshida, K. Tanaka, A. Fujimori, M. Okusawa, S. Wakimoto, K. Yamada, T. Kakeshita, H. Eisaki, S. Uchida, *Phys. Rev. B* **75**, 140503(R) (2007).
- [5] H. Alloul, J. Bobroff, M. Gabay, P.J. Hirschfeld, *Rev. Mod. Phys.* **81**, 45 (2009).
- [6] J.L. Tallon, J.W. Loram, *Physica C* **349**, 53 (2001) and the references cited herein.
- [7] A. Malinowski, M.Z. Cieplak, S. Guha, Q. Wu, B. Kim, A. Krickser, A. Perali, K. Karpinska, M. Berkowski, C.H. Shang, P. Lindenfeld, *Phys. Rev. B* **66**, 104512 (2002).
- [8] R.G. Buckley, M.P. Staines, E.M. Haines, M. Ziaei, B.P. Clayman, *Physica C* **235-240**, 1237 (1994).
- [9] G.V.M. Williams, J.L. Tallon, R. Meinhold, A. Jánossy, *Phys. Rev. B* **51**, 16503 (1995).
- [10] B. Nachumi, A. Keren, K. Kojima, M. Larkin, G.M. Luke, J. Merrin, O. Tchernyshöv, Y.J. Uemura, N. Ichikawa, M. Goto, S. Uchida, *Phys. Rev. Lett.* **77**, 5421 (1996).
- [11] T. Nakano, N. Momono, T. Nagata, M. Oda, M. Ido, *Phys. Rev. B* **58**, 5831 (1998).
- [12] G. Xiao, M. Cieplak, J.Q. Xiao, C.L. Chien, *Phys. Rev. B* **42**, 8752 (1990).
- [13] T. Adachi, S. Yairi, K. Takahashi, Y. Koike, I. Watanabe, K. Nagamine, *Phys. Rev. B* **69**, 184507 (2004).
- [14] M. Kofu, H. Kimura, K. Hirota, *Phys. Rev. B* **72**, 064502 (2005).
- [15] N. Ishikawa, N. Kuroda, H. Ikeda, R. Yoshizaki, *Physica C* **203**, 284 (1992).
- [16] H. Hiraka, D. Matsumura, Y. Nishihata, J. Mizuki, K. Yamada, *Phys. Rev. Lett.* **102**, 037002 (2009).
- [17] M. Zhiqiang, X. Gaojie, Y. Hongjie, W. Bin, Q. Xueyin, Z. Yuheng, *Phys. Rev. B* **58**, 15116 (1998).
- [18] G. Xiao, J.Q. Xiao, C.L. Chien, M.Z. Cieplak, *Phys. Rev. B* **43**, 1245 (1991).
- [19] D.C. Johnston, *Phys. Rev. Lett.* **62**, 957 (1989).
- [20] T. Nakano, M. Oda, C. Manabe, N. Momono, Y. Miura, M. Ido, *Phys. Rev. B* **49**, 16000 (1994).
- [21] S. Zagoulaev, P. Monod, J. Jégoudez, *Physica C* **259**, 271 (1996).
- [22] M.-H. Julien, T. Fehér, M. Horcatic, C. Berthier, O.N. Bakharev, P. Ségransan, G. Collin, J.-F. Marucco, *Phys. Rev. Lett.* **84**, 3422 (2000).